

# Effects of Frequency Variation at Inlet Flow on the Vortex Shedding Frequency Behind a Circular Cylinder

E. Yousefi-Rad<sup>1</sup>, M. Pasandideh-fard<sup>2</sup>

*In many applications, the flow past bluff bodies has a frequency nature (oscillated) and is not uniform. This kind of flow has some effects on the formation of vortex shedding behind bluff bodies. In this paper, the flow around a circular cylinder was numerically simulated. The effects of frequency variation at inlet flow on the vortex shedding frequency were investigated. The transient Two-Dimensional Navier-Stokes equations were employed to compute the unsteady laminar free stream flow over a circular cylinder. A time series analysis for the formations of vortex shedding behind the circular cylinder was performed under uniform (Frequency=0) and oscillated flows (Frequency=0.1, 1, 10, 60 and 100Hz) at Re=300. Then, the value of amplitude for one of the oscillated flows was changed. The global quantities such as drag coefficients and Strouhal number variables were compared for the above range of conditions for both uniform and oscillated flows. Results show that by increasing the inlet flow frequency, Strouhal number increases slightly and the oscillation amplitude of drag coefficient increases considerably. However, the mean sizes of drag coefficients do not vary in all computations. Also, the effect of variation in velocity amplitude on vortex shedding frequency and drag coefficient value was studied.*

## INTRODUCTION

The flow around a circular cylinder due to the complex nature of the flow remains a challenging problem in fluid mechanics today. Cross-flow normal to the axis of a stationary circular cylinder and the associated problems of heat and mass transport are encountered in a wide variety of engineering applications [1]. Vortex shedding in the wake behind circular cylinders has been the focus of attention in a number of experiments in recent years [2, 3, 4 and 5]. The occurrence of this flow phenomenon is due to instabilities and depends on the geometry of the bluff body and the Reynolds number; it has often been the cause of failure of flow-exposed structures in various fields of engineering. The non-dimensional shedding frequency, the Strouhal number,

is defined as:

$$St = \omega \frac{D}{U_{\infty}} \quad (1)$$

where  $\omega$  is the shedding frequency,  $D$  is the characteristic length and  $U_{\infty}$  is free stream flow velocity. Over a wide range of Reynolds numbers, the Strouhal number is constant, implying a linear relationship between shedding frequency and mean velocity. Due to the vortex shedding is highly affected by Reynolds number thus extensive review of the analysis of vortex shedding past steady circular cylinders was done. The major Reynolds regimes of vortex shedding are reported in Lienhard [6]. In particular, at  $Re = 5$ , the flow does not detach from the cylinder surface, so the fluid follows the cylinder contours. In the range  $5 \leq Re \leq 45$ , the flow separates from the back of the cylinder and the near wake is characterized by a symmetric pair of vortices. If  $Re$  is further increased, the wake becomes unstable and the vortices shed alternately from the cylinder sides. The wake is given by two vortices of

1. Ph.D. Candidate, Dept. of Mech. Eng., Ferdowsi University of Mashhad, Khorasan, Iran, Email: edris.yousefirad@gmail.com.

2. Associated Professor, Dept. of Mech. Eng., Ferdowsi University of Mashhad, Khorasan, Iran.

opposite sign (Vortex Street) and is laminar. In the range  $150 \leq Re \leq 300$ , although the boundary layer on the cylinder remains laminar, the wake becomes turbulent.

The vortex shedding is strong and periodic in the sub-critical range ( $300 < Re \leq 1.5 \times 10^5$ ) [5].

Due to these phenomena, the flow at  $Re=300$  was deeply considered in the analyses of this study. In addition to the familiar Kármán vortex street behind a stationary cylinder in a uniform stream, several other complex vortex patterns have been observed in the wakes of oscillating cylinders. There is a large body of literature on experimental studies of vortex wakes behind cylinders oscillating either perpendicularly to or in-line with the uniform stream [7]. An attempt at classifying such vortex patterns has been made by Williamson and Roshko [8], henceforth referred to as WR, using a symbolic code of letters and numbers that describes the combination of pairs and single vortices shed during each cycle of the forced oscillation of the cylinder. Another phenomenon that occurs in nature is oscillated flow that crosses over bluff bodies such as fans that provide periodic flow. In order to capture periodic vortex shedding only a few studies were done [9] in which the oscillated pressure was considered to simulate vortex shedding. In experimental studies, visualization techniques such as hot wire and Laser Doppler Velocimetry (LDV) are usually employed [10 and 11]. When a fluid flows around a bluff body, vortices are alternatively shed and a well known Karman vortex street is formed in the wake of the cylinder. Using the concept of curve fitting, correlations have been obtained for Strouhal number variation with Reynolds number [5]. In other works, the function of oscillated flow was optimized by using entropy flow theory and a better state of amplitude value for this vortex shedding simulation [12] was found.

### CHARACTERISTICS OF FLOWS OVER CIRCULAR CYLINDER

In this paper, the two-dimensional flow of an incompressible fluid around a circular cylinder was simulated in both uniform stream flow and oscillated flows at  $Re=300$ . Both experimental measurements and numerical computations have confirmed the onset of instability of the wake flow behind a cylinder beyond a critical Reynolds number, leading finally to a kind of periodic flow identified by definite frequencies, well-known in the literature as the Von Karman vortex street [13]. No slip condition is imposed as initial conditions. In case of laminar flow past cylinders with regular polygonal cross-section, the flow usually separates at one or more sharp corners of the cross-section geometry itself, forming a system of vortices in the wake on either side of the mid symmetry plane.

The mesh study was carried out for uniform inlet flow and the minimum grid nodes with the same values for Strouhal number and drag coefficient were selected for all numerical simulations. The code is validated with the Thompson's experimental data in uniform flow [14]. The vortex shedding taking place behind the circular cylinder has shown good accuracy with the experimental data. The code was extended to compute vortex shedding induced by inlet oscillated flow after validation. For the first step, the optimized number of nodes for grid independency is found. The numerical results from both uniform and fluctuating flow were compared. The global quantities such as drag coefficients, Strouhal number, drag coefficient and variables like stream function, vorticity have been obtained in oscillated flow in various frequencies (0,0.1,1,10,60 and 100Hz). Then, the results obtained for various values of amplitude of oscillation were compared with the result of uniform flow. It was found how vortex shedding characteristics were affected by the periodic incoming disturbances. Therefore, the results could be useful for calibrating the flow meter in unsteady flow measurement.

### GOVERNING EQUATIONS

The governing equation for Two-Dimensional cylindrical unsteady laminar incompressible flow is continuity (Equation 2) and Navier-Stokes equation as follows (Equations 3 and 4):

$$\frac{\partial}{\partial r}(ru) + \frac{\partial}{\partial \theta} = 0 \quad (2)$$

*R*-momentum:

$$\rho \left( \frac{\partial u}{\partial t} + u \frac{\partial u}{\partial r} + \frac{v \partial u}{r \partial \theta} \right) = -\frac{\partial p}{\partial r} + \frac{1}{r} \frac{\partial}{\partial r} \left( \mu r \frac{\partial u}{\partial r} \right) + \quad (3)$$

$$\frac{1}{r} \frac{\partial}{\partial \theta} \left( \frac{\mu \partial u}{r \partial \theta} \right) + \rho \frac{v^2}{r} + \frac{1}{r} \frac{\partial}{\partial r} \left( \mu r \frac{\partial u}{\partial r} \right) + \quad (4)$$

$$\frac{1}{r} \frac{\partial}{\partial \theta} \left\{ \mu r \frac{\partial}{\partial r} \left( \frac{v}{r} \right) \right\} - 2 \frac{\mu}{r^2} \left( \frac{\partial v}{\partial \theta} + u \right) \quad (5)$$

*θ*-momentum:

$$\rho \left( \frac{\partial u}{\partial t} + u \frac{\partial u}{\partial r} + \frac{v \partial u}{r \partial \theta} \right) = -\frac{1}{r} \frac{\partial p}{\partial \theta} + \frac{1}{r} \frac{\partial}{\partial \theta} \left( \mu r \frac{\partial v}{\partial r} \right) \quad (6)$$

$$+ \frac{1}{r} \frac{\partial}{\partial \theta} \left( \frac{\mu \partial v}{r \partial \theta} \right) + \frac{1}{r} \frac{\partial}{\partial r} \left( \mu \frac{\partial u}{\partial \theta} \right) + \frac{\mu \partial u}{r^2 \partial \theta} \quad (7)$$

$$\frac{1}{r} \frac{\partial}{\partial \theta} \left( \mu \frac{u}{r} \right) - \frac{1}{r} \frac{\partial}{\partial \theta} \left( \mu \frac{\partial u}{\partial r} \right) - \frac{1}{r^2} v \frac{\partial (r\mu)}{\partial r} - \frac{\rho uv}{r} \quad (8)$$

where  $u$  and  $v$  are velocity components in  $r$  and  $\theta$  direction. The second order upwind scheme was employed to discrete momentum equations which were solved implicitly. Computations have been carried out

for Reynolds numbers 300. The coupling between continuity and momentum equations was achieved with the SIMPLEC predictor-corrector algorithm of van Doormal and Raithby [15], which is an improved version of the SIMPLE algorithm. The velocity inlet condition was applied at the inlet and the pressure outlet was performed for the exit(Figure 1). The code was extended to compute vortex shedding induced by inlet oscillated flow after validation. The selected inlet velocity amplitude and frequency were defined as a variable function explained in next part.

**RESULTS AND DISCUSSIONS**

**a. Uniform flow over cylinder**

In order to obtain reliable and accurate results, it is important to choose the length and width of the computational domain and grid size carefully. The domain of computations was considered as C-Grid as shown in Figure 1. All the numerical simulations were carried out for a 1cm-diameter cylinder. The liquid was assumed water with constant 300K as temperature.

The mesh independency was studied for uniform inlet flow. Four number of grid nodes were selected and the results were compared for drag coefficient and Strouhal number (see Table 1).

Results show that the domain with 82500 grid nodes or higher have the same values for Strouhal number and drag coefficient. Considering this, 82500 grid nodes were selected for all the numerical simulation in this study. To validate the code, the

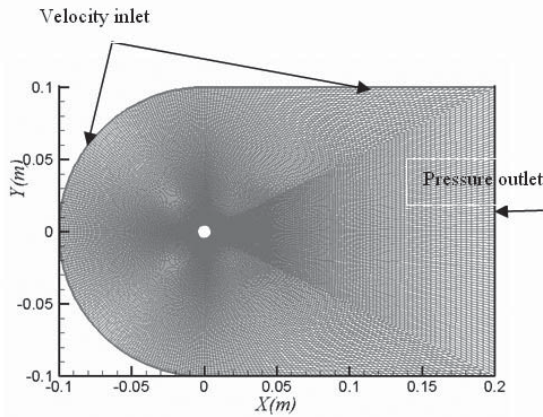


**Figure 1.** C-Grid domain used for computation.

**Table 1.** Computed drag coefficient and Strouhal number in four Number of Nodes.

Number of Nodes	$C_d$	Strouhal
28000	1.345	0.202
57500	1.353	0.204
82500	1.366	0.207
103000	1.366	0.207

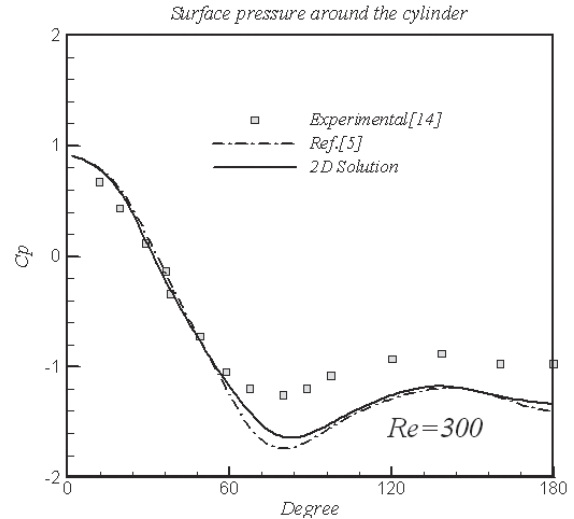


**Figure 2.** Comparison between numerical results and experimental data [14] for Pressure Coefficient versus angle of attack at  $Re=300$ .

vortex shedding was simulated for the uniform inlet flow and the results were compared with a case for which measurements were available in experimental data[14]. So, the flow with Reynolds number equal to 300 was chosen. Further, the results were compared with corresponding numerical predictions presented in Ref. [5]. Figure 2 shows that the agreement between the measurement data and the computational results is excellent in the accelerating flow zone covering the front part of the cylinder.

But large differences of the order of 14% are observed for the suction peak and the so-called base pressure in the rear part of the cylinder. This contradiction may be attributed mainly to the inaccurate prediction of location of the unsteady flow separation point on the cylinder surface. However, the predictions obtained in this work are better compared with those given in Ref.[5] in which a deviation of at least 20% with data was reported.

**b. Oscillated flow on a circular cylinder**

The code was extended to compute vortex shedding which is induced with oscillated flow. The selected inlet velocity amplitude and frequency were defined as the

**Table 2.** Computed times for symmetry and Asymmetry vortex shedding.

Frequency	Symmetry (sec)	Asymmetry (sec)
0	$t < 8.5$	$15.0 < t$
0.1	$t < 8.6$	$15.3 < t$
1	$t < 8.6$	$15.6 < t$
10	$t < 9.0$	$16.0 < t$
60	$t < 9.5$	$16.5 < t$
100	$t < 10.0$	$17.0 < t$

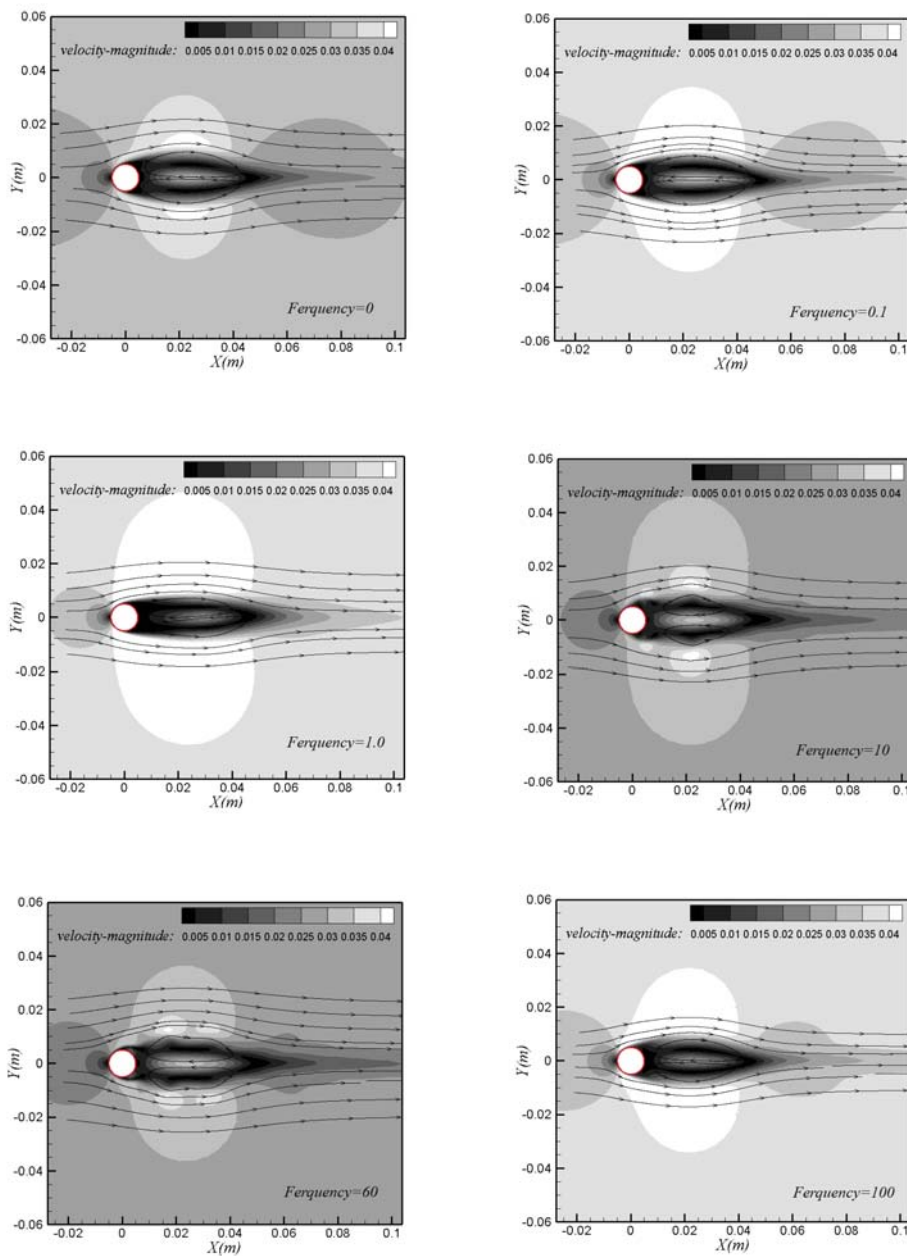


**Figure 3.** Contours of velocity magnitude at 7.5 seconds for inlet flow with various frequencies.

below function:

$$U = 0.03144 + 0.007536 \sin \omega t \quad (9)$$

where  $U$  is velocity along  $x$  axis,  $\omega$  is frequency and  $t$  is time. The value of  $0.03144 \text{ m/s}$  is the velocity of water at  $\text{Re}=300$  calculated from the below equation:

$$\text{Re} = \frac{U_{\infty} D}{\nu} \quad (10)$$

A time series analysis was performed for inlet flow with various frequencies. In Table 2, computed times for formation vortices are presented.

These results reveal that before 8.5 seconds vortices are symmetric for all investigated frequencies. In addition, when the incoming flow frequency increases, the time remaining symmetry flow increases slightly. Besides, for asymmetry flow required time for forming asymmetry vortices increases. Due to these reasons, two times were selected for the analysis of vortex shedding behavior: (a) 7.5 seconds for symmetry vortices and (b) 17.5 seconds for asymmetry vortices.

Figure 3 shows the velocity magnitude contours and stream lines for various inlet flow frequencies at

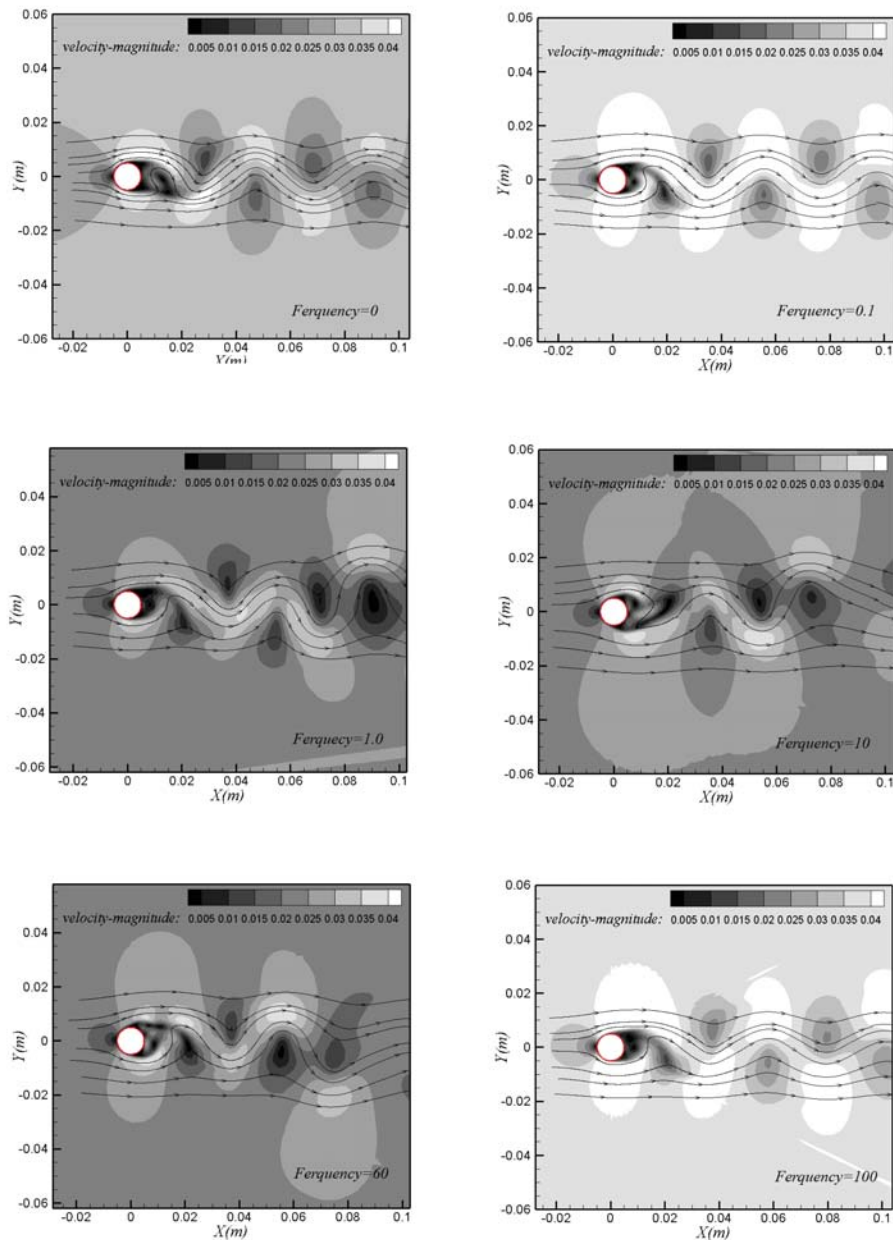


Figure 4. Contours of velocity magnitude at 17.5 seconds for inlet flow with various frequencies.

7.5 seconds. It can be seen that all the vortices are symmetric. In this state, the results are checked in 25 frequencies (between 0 and 100 Hz) and it showed that increasing the inlet flow frequency does not have a significant effect on the formation of vortices. But in this interval, 10Hz and 60Hz of frequency had some swing. Finally, when frequency increased in inlet flow, it caused the vortices to decrease slightly, at the end as shown for frequency of 100Hz.

Asymmetry vortices are shown in Figure 4 for various frequencies of inlet flows. Formations of vortices

and stream lines in different frequencies at 17.5 seconds were simulated. Although the number of vortices are the same (had different stream lines in frequency of 10Hz), the size of the vortices decreases by increasing the inlet flow frequency and the slope of stream line increases at high frequencies.

Figure 5 shows the variation between drag coefficient and time for different inlet flow frequencies. It can be seen that in low frequencies the oscillation amplitude of drag coefficient is relatively low and oscillates between 1.1 to 1.4. For flow with frequency=1,

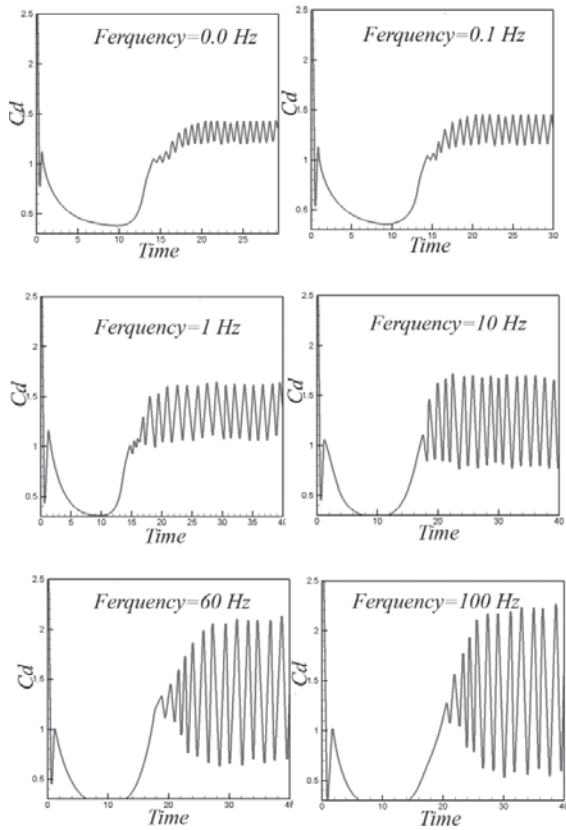


Figure 5. variation between drag coefficient and time for different inlet flow frequencies.

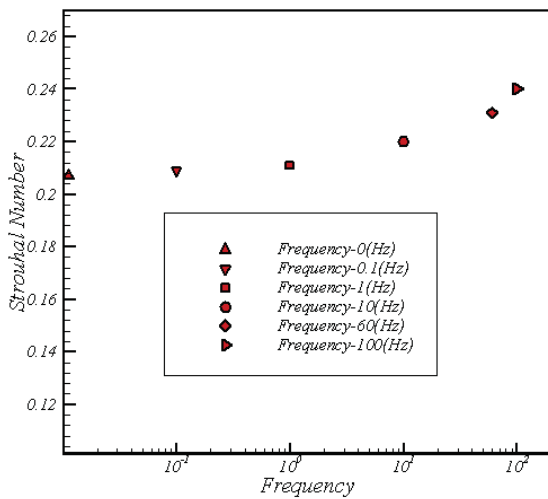


Figure 6. Variation between Strouhal number and inlet flow frequencies.

this amplitude increases slightly and drag coefficient oscillates between 1 to 1.6. At frequency=10, the drag coefficient amplitude oscillates between 0.8 to 1.7. For both inlet flow frequencies 60 and 100, the behavior of drag coefficient oscillations is approximately the same. The amplitude of oscillation in these cases is

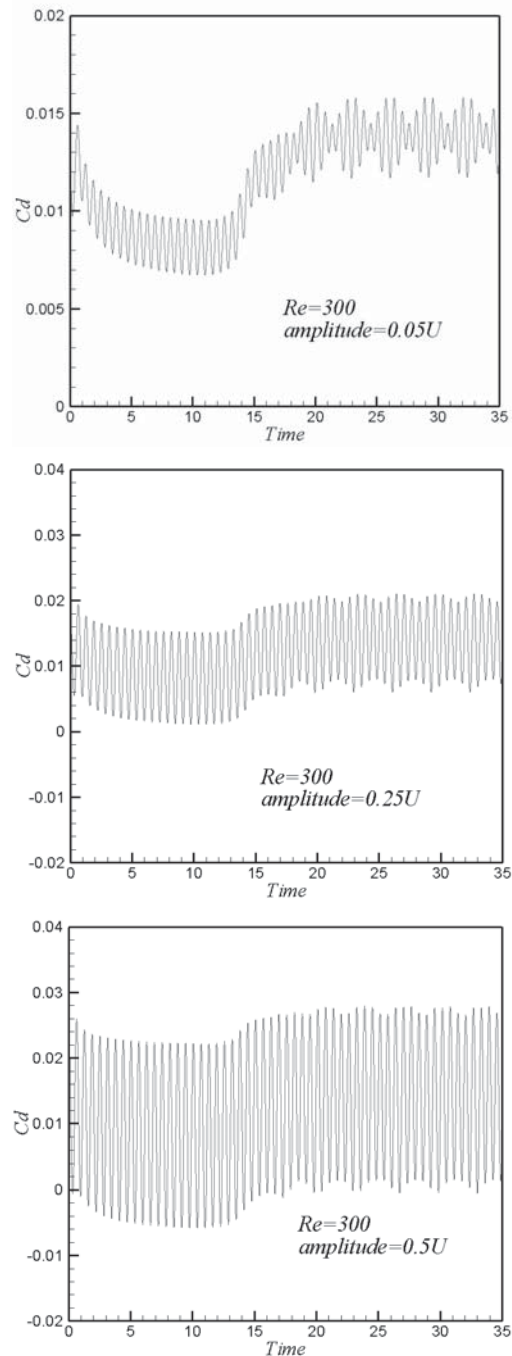


Figure 7. Variation between drag coefficient and time for different amplitude.

between 0.5 to 2.1. Although the amplitude of drag coefficient increases significantly, the mean average of drag coefficient is not affected by variation of inlet flow frequency and it is approximately constant. The values of Strouhal number for inlet flow with various frequencies were calculated (see Figure 6). It is clearly understood that Strouhal number increases slightly with an increase in inlet flow frequency. It can be seen that the numerical results are approximately accurate

for unsteady periodic flows when a proper grid and time step size are used.

Figure 7 shows the variation of drag coefficient with passing time. The value of amplitude for one of the oscillated flows such as the number of frequency equal to 10Hz was changed. It can be seen that as the value of amplitude varies considerably, the mean value of drag coefficient is not changed. However, the amplitude of drag coefficient frequencies varied significantly. It is interesting that the drag coefficient amplitude variations decrease for higher values of inlet flow amplitudes.

### CONCLUDING REMARKS

Using transient two-dimensional Navier-Stokes equation vortex shedding phenomenon was simulated. The flow behavior behind a circular cylinder and wake structure was investigated for oscillated flow with various frequencies by using a second order upwind implicit scheme. A-time series of analysis was performed to compare vortex behavior behind circular cylinder for various inlet velocity frequencies. Results show that by increasing the frequency of the inlet flow, the Strouhal number is increased slightly. Although the amplitude of the drag coefficient increases dramatically, the mean average of the drag coefficient is not affected by variation of the inlet flow frequency and it has an approximately constant value.

### REFERENCES

1. Zdravkovich M., *Flow Around Circular Cylinders*, 1, Oxford Science Publication, (1997).
2. Williamson C., "Vortex Dynamics in the Cylinder Wake", *Annual Review of Fluid Mechanics*, **28**, (1996).
3. Frankie R., Rodi W. and Schunung B., "Numerical Calculation of Laminar Vortex Shedding Flow Past Cylinders", *Journal of Wind Engineering and Industrial Aerodynamics*, **35**, (1990).
4. Young D.L., Haung J.L. and Eldho T.I., "Simulation of Laminar Vortex Shedding Flow Past Cylinders Using a Coupled BEM and FEM Model", *J. Comput. Methods Appl. Mech. Engrg.*, **190**, (2001).
5. Rajani B.N., Kandasamy A. and S. Majumdar S., "Numerical Simulation of Laminar Flow Past a Circular Cylinder", *J. Applied Mathematical Modelling*, **33**, (2009).
6. Lienhard J., "Synopsis of Lift, Drag and Vortex Frequency Data for Rigid Circular Cylinder", *Washington State University, College of Engineering, Research Division Bulletin 300*, (1966).
7. Khalak A., Williamson C.H.K., "Motion Forces and Mode Transitions in Vortex-Induced Vibration at Low Mass-Damping", *J. Fluids Structure*, **13**, (1999).
8. Williamson C.H.K., Roshko A., "Vortex Formation in the Wake of an Oscillating Cylinder", *J. Fluids Structure*, **2**, (1988).
9. Frank S., Xin F. and Ying C., "Effect of Pressure Unsteadiness on Vortex Shedding Frequency From Dual Bluff Body", Ph.D. Thesis, Technical University of Karlsruhe, Germany, (2000).
10. Williamson C.H.K., "Vortex Dynamics in the Cylinder Wake", *Annu. Rev. Fluid. Mech., Annual Reviews Inc.*, (1996).
11. Bearman, "Vortex Shedding from Oscillating Bluff Bodies", *Ann. Rev. Fluid Mech.*, **16**, PP 195-222(1984).
12. Yousefi-Rad E., Pasandideh-fard M., "Numerical Simulation of Unsteady Flow Around Circular Cylinder With Computing Entropy Generation And Vortex Shedding", *ASME 2010*, Vancouver, British Columbia, Canada, (2010).
13. Rajani B.N. , Gopal Lanka H. and Majumdar S., "Laminar Flow Past a Circular Cylinder at Reynolds Number Varying from 50 to 5000", *NAL PD CF 0501*, (2005).
14. Thompson M., Hourigan K. and Sheridan J., "Three-Dimensional Instabilities in the Wake of a Circular Cylinder", *Exp. Thermal Fluid Science*, **12**, (1996).
15. Vandoormaal J.P., Raithby G.D., "Enhancements of the SIMPLE Method for Predicting Incompressible Fluid Flows", *Numer. Heat Transfer*, **7**, PP 147-163(1984).